DIGITAL POWER SUPPLY FOR AIR CORE MAGNET

S. H. Jeong [#], K. H. Park, D. E. Kim, J. H. Choi

Pohang Accelerator Laboratory, POSTECH, Pohang, Kyungpook 790-784, Korea

Abstract

This paper presents the magnet power supply (MPS) for air-core corrector magnet at the Pohang Light Source. The required current to energize the magnet was ±5 A. The MPS has been implemented using the digital signal processing technology and shows the high stability and other good responses. The stability of the MPS was about ~2 ppm in short and long term, respectively. Various experimental results such as stability, bandwidth and simulation are given in this paper.

INTRODUCTION

The MPS are required of accelerator facilities to deflect electron beam trajectory. For these applications, the MPS should have the high precision and stability for stringent specification of storage ring.

The digital signal processor (DSP) had been developed primarily for application in various digital signal processing. The DSP was suitable for implementing the complicated algorithms such as feedback control, digital filters, and so on. And it includes many hardware functions to make it easy to interface the peripherals chips by the SPI, CAN, RS232C, etc. Thus the application areas of the DSP become wider day by day, especially in power conversion systems - power supply, UPS, inverter, etc. [1].

Nowadays the DSP combining with the FPGA were adapted for construction of the MPS with high performance in many laboratories and industries. In order to achieve requirement of the high stability on output current, the MPS using the DSP TMS320F2808 from the Texas Instrument was developed.

Conventionally, the regulation circuits of the MPS are realized using analog circuit technique. The analogue controller is easy to implementation and good for simple circuits. With a good DAC and the other circuits, a high stability MPS can be archived. But, analog control technique has demerits in complex circuit design, low reliability, non-flexibility, and higher manufacturing cost.

In this paper, we present the design scheme and measured results of the fully digital-controlled high precision MPS for air core magnet of the Pohang Light Source.

AVERAGE CURRENT MODE CONTROL

The control of a switching mode power supply can be analysed using either the average current or peak current mode operations. For the peak current mode control, the instantaneous peak current of the inductor, which regulates the output current, is sensed and used to determine the duty ratio of the PWM. The duty ratio determined from the measured instantaneous peak current

Other

is quite fluctuating, and the peak current mode control is not suitable for a precision MPS for accelerator. For the average current mode (ACM) control [2], the load current is sensed and averaged for a given control loop duration, compared with the reference value to obtain the current error, and the current error is fed into the compensator in the control loop. Because the load current is averaged over the control loop duration, the control loop has a better noise immunity, higher current loop gain, no stability problem when the duty cycle is above 0.5. These appealing features have contributed to its popularity in today's DC-DC converters. A schematic diagram of buck mode MPS using the ACM control is shown in Fig.1. Here, D is the steady state duty ratio of the IGBT control signal, $H(s)$ is the gain of current sensor, and $G_c(s)$ is the proportional and integral (PI) compensator for load current regulation.
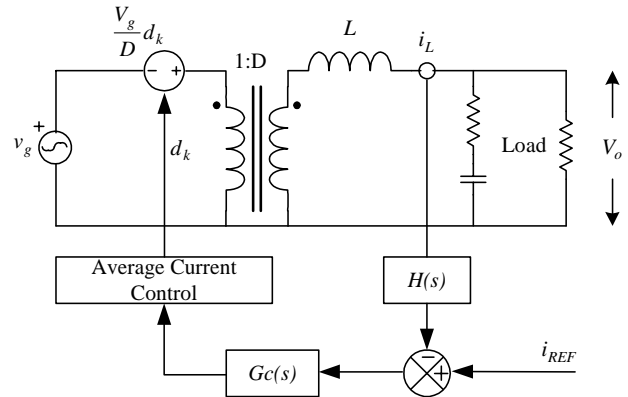
Figure 1: A schematic diagram of bucked mode MPS using the ACM control.

For an analysis of the MPS, we assume that the current through the filter capacitor is much smaller than the load current and the converter operated at a continuous conduction mode. Then the inductor current is given by the following equations:

$$L\frac{di_L}{dt} = V_g - V_o \quad \text{for} \quad t_k \le t < t_k + d_k T_s \qquad (1)$$

$$L\frac{di_L}{dt} = -V_o \quad \text{for} \quad t_k + d_k T_s \le t < t_{k+1} \qquad (2)$$

Thus the initial inductor current at the $(k+1)th$ switching cycle can be written as

$$i_L(k+1) = i_L(k) + \frac{V_g(k) - V_o(k)}{L}d(k)T_s - \frac{V_o(k)}{L}(1 - d(k))T_s \quad (3)$$

where d_k is the duty ratio function of the PWM and T_s is the switching period. In a steady state operation, the inductor current should follow the reference current $i_{REF}(k)$, i.e., $i_{REF}(k) = i_L(k)$.

From (3), the duty ratio in k th switching period is given by

$$d(k) = \frac{[i_{REF}(k+1) - i_{REF}(k)]L/T_s}{V_g(k)} + \frac{V_o(k)}{V_g(k)} \qquad (4)$$

Then, the time averaged load current $<i_L>$ becomes

$$<i_L> = \frac{1}{T_s}\int_t i_L dt \quad \text{for } t_k \leq t < t_k + T_s. \qquad (5)$$

During each switching period, the averaged load current $<i_L>$ was calculated in DSP using the digitized load current and the error from $i_{REF}(k)$ was fed into the PI compensator.

SYSTEM CONFIGURATION

The system configuration of the designed MPS is shown in Fig. 2. Current feedback and input voltage feed-forward control schemes are applied to improve the output current stability. We used the DSP TMS320F2808 to control the overall power supply system. The controllability of the TMS320F2808 with the micro-edge positioning technology[3] was less than 10 ppm, which satisfied the required accuracy for the MPS. The IRF540 FETs from International Rectifier Co. used for switching elements.
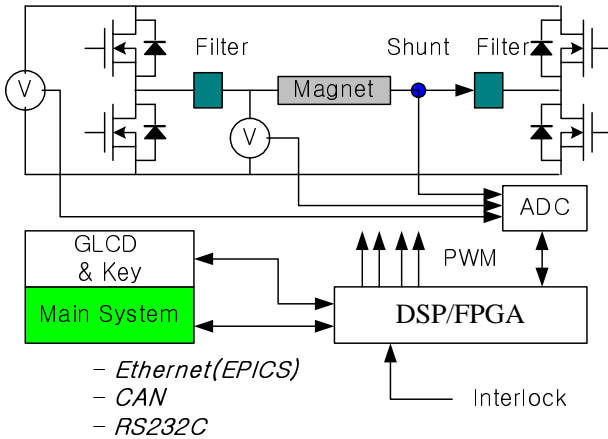
Figure 2: Functional Block Diagram.

The output filter is composed of conventional R-L-C filter which includes an R-C damping circuit to make good filter response.
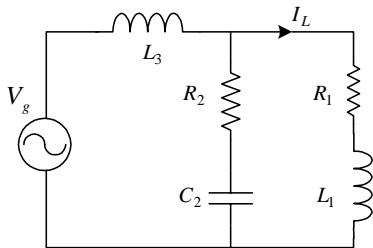
Figure 3: Equivalent circuit of output filter and load magnet.

Other

The output filter and load magnet were modelled as shown Fig. 3, where the load magnet was modelled with R_1 and L_1, and the filter circuit consisted of C_2, R_2 and L_3. The implemented output filter had more components, other than the one shown Fig. 3, but the values of other components are so small that the effects of these components could be ignored.

The transfer function $G_p(s)$ of the circuit in Fig. 3 is

$$G_p(s) \equiv \frac{I_L(s)}{V_g(s)} = \frac{b_1 S + 1}{a_3 S^3 + a_2 S^2 + a_1 S^1 + R_1} \qquad (6)$$

where $a_1 \equiv L_1 + L_3 + R_1 R_2 C_2$, $a_2 \equiv R_2 C_2 L_1 + L_3 R_1 C_2 + L_3 R_2 C_2$, $a_3 \equiv C_2 L_1 L_3$, and $b_1 = C_2 R_2$. The control loop for the designed MPS is given in Fig. 4. It does not contain any voltage feedback or reference feed-forward. The coefficients of PI compensator $G_c(s)$ were determined directly using the characteristic equation of the control loop. The closed-loop control system for the PPS is given Figure 4.
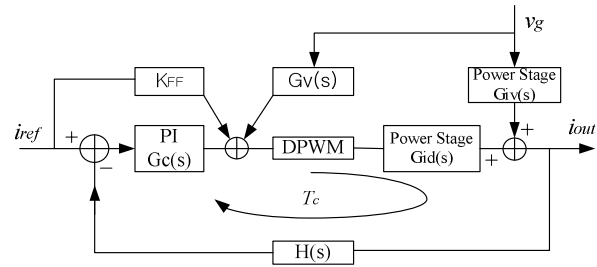
Figure 4: Block diagram of complete current loop system.

The closed-loop transfer function of the power supply is given by:

$$i_{out}(s) = i_{ref}(s)\left(\frac{G_c G_{id}}{1+T_c} + \frac{K_{FF}G_{id}}{1+T_c}\right) + v_g(s)\left(\frac{G_{iv}}{1+T_c} + G_v\frac{G_{id}}{1+T_c}\right)$$

while current loop gain, T_c is $T_c(s) = G_c(s) \bullet G_{id}(s) \bullet H(s)$.

The sensed link voltage was used to modify the duty cycle. The updated duty cycle is expressed as $d_{update}(k) = d(k) + G_v\Delta d(k)$, where $\Delta d(k) = (V_{ref} - v_{in}(k))/V_{ref}$ and G_v is the feed-forward gain.

The output current was measured using a shunt resistor and the voltage developed at the shunt resistor was converted into a digital signal by the two AD977As analogue-to-digital converter (ADC) from Analog Devices. For each control update time, each ADC digitised the output current ten times. The outputs of both ADCs were summed and averaged to reduce the system noise. The switching frequency was 25kHz. The overall control loop was updated for every 200 μs using the timer Interrupt of the TMS320F2808. Both key scan and the LCD display operations were carried out at the base routine to avoid any serious control timer interrupt.

EXPERIMENTAL RESULTS

A 24 hours long term current stability was measured using the HP3458A digital voltmeter from Agilent Co, and the results are shown in Fig. 5. The stability of load current was less than 2 ppm at 4.4 A output current.
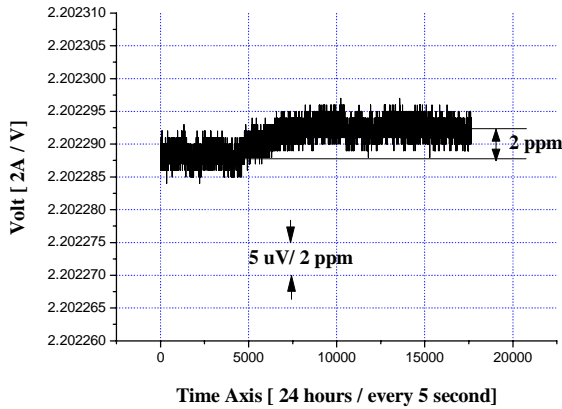
Figure 5: Current stability at load current of 4.4 A.
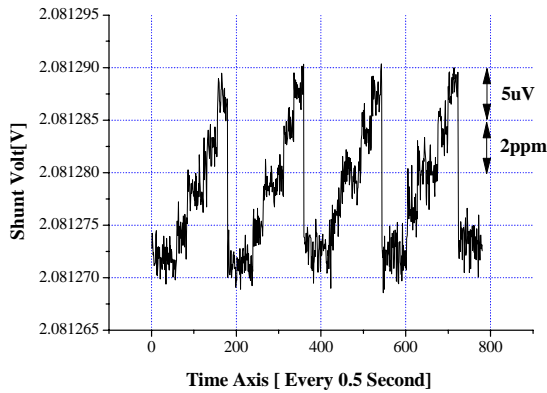
Figure 6: Current control step resolution.

Fig 6 shows the current control step resolution and the resolution step is 1 ppm. It shows the good iteration.
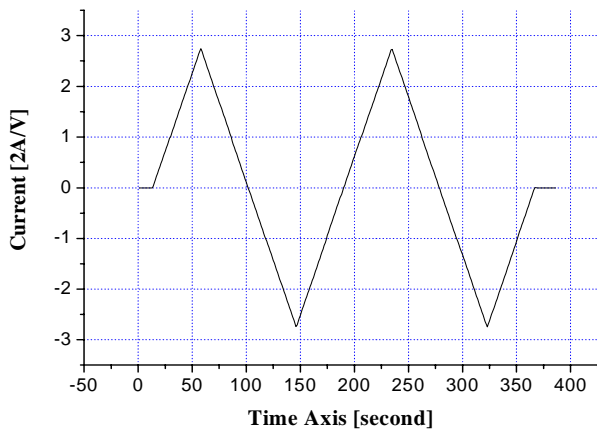
Figure 7: Current ramping test.

Fig 7 shows the current ramping test result. Ramping test is done from -2.75A to 2.75A. It shows the good performance of iteration and accuracy.
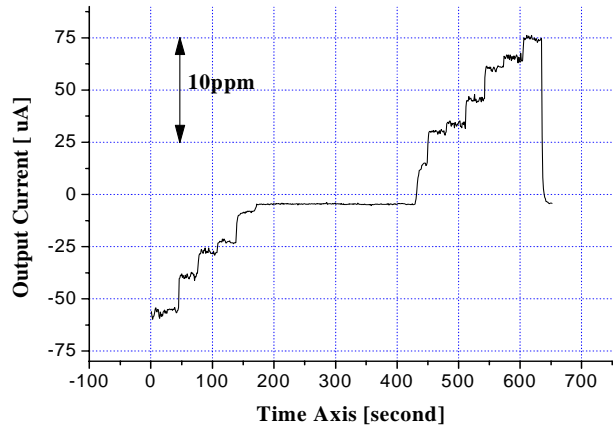
Figure 8: Zero current crossing characteristics of polarity change   .

Fig 8 shows the transition characteristics when polarity changes. It shows the good controllability at near the zero current from -60 µA to 75 µA. It is controlled by 1 ppm step.

CONCLUSIONS

This paper described the DSP-controlled Bipolar power supply for the air-core magnet. The designed digital controller includes a current feedback loop, which was applied by the PI control scheme with 30kHz updating speed. From the experimental results with assembled power supply, high stability and high accuracy step control were achieved. The short term stability is about ~1.8 ppm and 24 hour long term stability is about 2 ppm.

REFERENCES

[1] Shyh-Shin Liang, "DSP control of a resonant switching high-voltage power supply for X-ray generators," PEDS' 01, Indonesia, vol. 2, p. 522.
[2] G. Garcera, E. Figueres, M.Pascual and J.M. Benavent, "Analysis and design of a robust average current mode control loop for parallel buck DC-DC converters to reduce line and load disturbance", IEE Proc. Electr. Power appl. Vol. 151, No.4, July 2004, p. 414.
[3] Texas Instruments Co., www.ti.com

Other